

Partitioned Fitting and DC Correction in Transmission Line/Cable Models

M. Cervantes, I. Kocar, J. Mahseredjian, and A. Ramirez

Abstract--This paper presents further details of a previously proposed improved fitting procedure for transmission line/cable propagation functions, in which low frequency samples are given special attention. In the proposed approach, the frequency bandwidth is partitioned. At the first stage the fitting is performed for a high frequency band by excluding frequencies samples close to DC. The second stage finds a correction term for those excluded samples. This procedure achieves improved accuracy for transmission lines and cables used for HVDC transmission. The new approach complements the prevailing Universal Line Model (ULM) by avoiding numerical instabilities due to large residue/pole ratios while delivering accurate DC response. Two test cases are used to demonstrate the advantages of the new approach.

Keywords: Frequency dependent line models, electromagnetic transients, HVDC transmission lines.

I. INTRODUCTION

THE transient analysis of DC transmission lines has become of special interest with the increasing number of planned and installed HVDC systems [1]-[4]. The transmission line models for the simulation of such systems require covering a wide range of frequencies including those very close to DC.

This paper is based on the usage of the universal line model (ULM) [5] approach for modeling HVDC lines. Numerical implementation of ULM in EMT-type programs relies on representing line functions, i.e., propagation function (\mathbf{H}) and characteristic admittance (\mathbf{Y}_c) by rational function approximations, i.e., partial fractions, which are provided by existent curve fitting techniques [6]. One practice to capture the DC response in the ULM is to specify a very low frequency for fitting \mathbf{H} and \mathbf{Y}_c . However, this approach often leads to incorrect solutions for the DC steady-state voltages and currents due to generally poor DC fitting [7]-[8]. Moreover, resulting large residue/pole ratios and opposing signs from different modal groups in the fitting of \mathbf{H} , may cause numerical stability problems in time domain simulations [8]-[10]. The frequency dependent cable model (FDCM)

presented in [11] proposes a new method for correcting cases with numerical problems due to large residue/pole ratios. In FDCM, the large ratios are avoided by decomposing the propagation function \mathbf{H} into grouped modal contributions. The modal contribution groups are smooth functions of frequency and are fitted in phase domain. However, when this approach is applied to aerial lines, the problem of poor fitting at low frequencies is even more emphasized.

The method presented in [8], maintains a low frequency representation of the line model by using an additional low-order fitting function that compensates fitting errors at low frequencies. But this approach still requires a large frequency fitting range and may cause large residue/pole ratios that can produce numerical instabilities in time domain computations.

The fitting procedure of ULM can be modified [7] by forcing the exact DC response of \mathbf{H} in the rational approximation. However, this modification requires an additional optimization step of residues to reduce the acquired high-frequency errors.

In [9] the fitting approach of FDCM is extended by using a two-stage fitting method in which low frequency samples are given special attention. The first stage performs fitting by excluding very low (close to DC) frequency samples. The second stage finds a correction function for the initially excluded samples close to DC. This approach avoids large residue/pole ratios occurring in the classic ULM. This approach is called Frequency Dependent Model with DC correction (FDM/DC).

This paper provides more details on the fitting process presented in [9]. In addition, two new test cases are used in this paper to demonstrate advantages for accurately computing DC steady-state waveforms and preserving numerical stability.

II. REVIEW OF LINE/CABLE MODELING

A. Main Equations in Frequency Domain

A power line/cable system of length L formed by N conductors is presented in Fig. 1. Based on the current directions in Fig. 1, the frequency domain voltages and currents at both ends can be related using

$$\mathbf{I}_k = \mathbf{Y}_c \mathbf{V}_k - \mathbf{H}(\mathbf{I}_m + \mathbf{Y}_c \mathbf{V}_m) \quad (1)$$

$$\mathbf{I}_m = \mathbf{Y}_c \mathbf{V}_m - \mathbf{H}(\mathbf{I}_k + \mathbf{Y}_c \mathbf{V}_k) \quad (2)$$

where \mathbf{I}_k and \mathbf{I}_m are the vectors of injected currents, and \mathbf{V}_k and \mathbf{V}_m correspond to nodal voltage vectors. \mathbf{H} and \mathbf{Y}_c are defined by:

$$\mathbf{H} = e^{-\Gamma L} \quad (3)$$

$$\mathbf{Y}_c = \Gamma \mathbf{Z}^{-1} \quad (4)$$

M. Cervantes, I. Kocar and J. Mahseredjian are with the Department of Electrical Engineering, Polytechnique Montreal (Quebec), Canada. (e-mail: miguel.cervantes-martinez@polymtl.ca, ilhan.kocar@polymtl.ca, jean.mahseredjian@polymtl.ca).

A. Ramirez is with CINVESTAV Campus, Guadalajara 45019, Mexico (e-mail: abner.ramirez@cinvestav.mx).

Paper submitted to the International Conference on Power Systems Transients (IPST2019) in Perpignan, France, June 16-20, 2019.

where $\Gamma = \sqrt{\mathbf{YZ}}$, with \mathbf{Z} and \mathbf{Y} corresponding to the per unit length series impedance and shunt admittance matrices, respectively. Both \mathbf{Z} and \mathbf{Y} can be numerically obtained from the geometry and the electrical parameters of the line.

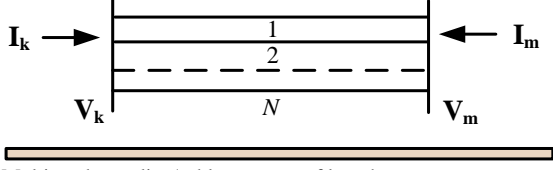


Fig. 1. Multiconductor line/cable segment of length L .

B. Universal Line Model (ULM)

In the ULM, \mathbf{H} is first diagonalized via modal decomposition [5]. Then, poles and delays are identified by fitting each mode. Modal delays have close values and are grouped [13]. Once the poles and delays are known, the matrix of residues is obtained by solving an overdetermined problem [5]. Thus, the propagation function \mathbf{H} is approximated in the following state space form:

$$\mathbf{H} \cong \sum_{i=1}^{N_{gr}} \left(\sum_{m=1}^{M_i} \frac{\mathbf{R}_{i,m}}{s - p_{i,m}} e^{-s\tau_i} \right) \quad (5)$$

where N_{gr} is the number of modal propagation groups, M_i is the order of the approximation for the i th modal group, $p_{i,m}$ represents its m th pole, $\mathbf{R}_{i,m}$ corresponds to the matrix of residues and τ_i is the time delay associated with the velocity of the i th modal group.

The characteristic admittance \mathbf{Y}_c is approximated directly in phase domain by:

$$\mathbf{Y}_c \cong \mathbf{G}_0 + \sum_{i=1}^{N_y} \frac{\mathbf{G}_i}{s - q_i} \quad (6)$$

where N_y is the order of approximation, q_i represents the i th fitting pole, \mathbf{G}_i is the corresponding matrix of residues, and \mathbf{G}_0 is a constant matrix representing the limit of \mathbf{Y}_c when $s \rightarrow \infty$.

C. Frequency-Dependent Cable Model (FDCM)

Although the ULM is applicable for most line/cable configurations, it generates unstable models in some cases [11]. The origin of the problem relies on the fitting of \mathbf{H} and can be explained as follows. Equation (5) contains multiples delay groups and it is solved using least squares method. The only criterion is the minimization of the difference between the fitted and the actual responses. Even though \mathbf{H} can be accurately fitted by combining the multiple delay groups, the rational approximation of separate delay groups does not necessarily match the actual modal contributions. As a result, the solution of (5) may result with delay groups having high residue/pole ratios. This may lead to numerically unstable models in the time domain solution.

Idempotent models also perform fitting through decomposition [12] but the non-smooth behavior associated with similar eigenvalues was overlooked. Moreover, it divides modal contributions into eigenvalues and idempotent matrices

which can reduce the efficiency of models due to cascaded convolutions in time domain.

The objective of the FDCM [11] is to properly account for modal contributions in the fitting of \mathbf{H} . In FDCM, similar eigenvalues of \mathbf{H} and their corresponding eigenvectors are grouped by summing them, and a single time delay is assigned to the group. The modal contribution groups are smooth functions of frequency. Hence, the propagation function matrix becomes

$$\mathbf{H} \cong \sum_{i=1}^{N_{gr}} \hat{\mathbf{H}}_i e^{-s\tau_i} \quad (7)$$

where N_{gr} is the number of modal contribution groups. The fitting of the propagation function is performed on each modal contribution group to obtain poles and residues simultaneously, and consequently, the high residue/pole ratios appearing in the ULM are eliminated. A common set of poles is used for each $\hat{\mathbf{H}}_i$ and the exponential time delay τ_i factor is removed prior to fitting to give

$$\hat{\mathbf{H}}_i \approx \sum_{m=1}^{M_i} \frac{\mathbf{R}_{i,m}}{s - p_{i,m}} \quad (8)$$

III. FDM/DC APPROACH

To increase the precision in the fitting of \mathbf{H} at frequencies close to DC, a two-stage fitting method is proposed in [9], which is called FDM/DC. In this approach, the frequency band is partitioned to relax fitting, and a correction term is found afterward. It has been reported in [14]-[15] that partitioning the frequency band improves fitting precision. In this section, this paper reviews the fitting technique presented in [9] and provides additional equations to clarify the final step of the fitting procedure of \mathbf{H} .

In the FDM/DC [9], the propagation function \mathbf{H} is fitted (see Fig. 2) using the following steps.

In the first step the frequency range is divided into low frequency (LF) and high frequency (HF) sections (ranges). Typically, the LF section is between 0.001 to 1 Hz and the HF section is between 1 Hz to 1 MHz.

In the second step, the fitting of HF, is performed to obtain $\tilde{\mathbf{H}}_{HF}$ (poles and residues). The rational approximation can be obtained by using either the FDCM or ULM approach, to give

$$\tilde{\mathbf{H}}_{HF} \cong \sum_{i=1}^{N_{gr}} \left(\sum_{m=1}^{M_i} \frac{\mathbf{R}_{i,m}}{s_{HF} - p_{i,m}} e^{-s_{HF}\tau_i} \right) \quad (9)$$

where $s_{HF} = j\omega_{HF}$.

The third step evaluates the fitted function $\tilde{\mathbf{H}}_{HF}$ for the LF range. The resulting error of fitting $\Delta\mathbf{H}_{LF}$ is given by

$$\Delta\mathbf{H}_{LF} = \mathbf{H}_{LF} - \tilde{\mathbf{H}}_{HF}(s_{LF}) = \mathbf{H}_{LF} - \tilde{\mathbf{H}}_{LF} \quad (10)$$

where $s_{LF} = j\omega_{LF}$, and \mathbf{H}_{LF} and $\tilde{\mathbf{H}}_{LF}$ are respectively the analytical and fitted propagation function at low frequencies.

The fourth step calculates the rational approximation $\Delta\tilde{\mathbf{H}}_{LF}$ for $\Delta\mathbf{H}_{LF}$. In the LF range, the propagation function behaves flat and the impact of time delay is negligible; thus,

an arbitrary time delay can be removed prior to fitting. In [9], it is proposed to use the delay associated to the first modal group, i.e. τ_1 , (labelled as delay 1 assuming that delays are sorted). Then, $\Delta\tilde{\mathbf{H}}_{LF}$ is computed as follows

$$\Delta\tilde{\mathbf{H}}_{LF} \cong \sum_{k=1}^{M_{DC}} \frac{\mathbf{R}_{DC,k}}{s_{LF} - p_{DC,k}} e^{(-s_{LF}\tau_1)} \quad (11)$$

where M_{DC} is the order of approximation, and \mathbf{R}_{DC} and p_{DC} are respectively the residues and poles obtained at the LF section, i.e. the DC correction terms.

The fifth step obtains the final rational approximation by combining the fitted functions given by (9) and (11):

$$\mathbf{H} \approx \tilde{\mathbf{H}}_{HF} + \Delta\tilde{\mathbf{H}}_{LF} \quad (12)$$

In this step, the DC correction terms in (11) are added to the first group in (9). Thus, the first modal group $\tilde{\mathbf{H}}_1$ is now obtained as

$$\tilde{\mathbf{H}}_1 = \left(\sum_{m=1}^{M_1} \frac{\mathbf{R}_{1,m}}{s - p_{1,m}} + \sum_{k=1}^{M_{DC}} \frac{\mathbf{R}_{DC,k}}{s - p_{DC,k}} \right) e^{(-s\tau_1)} \quad (13)$$

and the final propagation function is given by

$$\mathbf{H} \approx \tilde{\mathbf{H}}_1 + \sum_{i=2}^{N_{gr}} \left(\sum_{m=1}^{M_i} \frac{\mathbf{R}_{i,m}}{s - p_{i,m}} e^{(-s\tau_i)} \right) \quad (14)$$

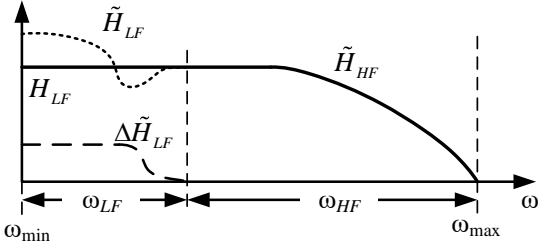


Fig. 2. Illustration of the FDM/DC approach for one entry of \mathbf{H} , i.e. H .

The approach detailed above allows achieving more accurate fitting at low frequencies. In addition, partitioning and reduced frequency ranges help avoiding pairs with large residue/pole ratios and consequently avoiding numerical instabilities that may occur in the classic implementation of ULM, regardless the integration method.

IV. NUMERICAL EXAMPLES

This section verifies the FDM/DC approach proposed in [9] through two new cases of study by showing details in both DC fitting and time-domain results. The impact of improving the fitting of \mathbf{H} at low frequencies in time-domain simulations is analyzed via transient studies.

A. AC and DC Lines in Parallel

This example considers the 220-km AC and DC transmission lines running in parallel with 80 m separation from each other, see Fig. 3. For this line, \mathbf{H} is fitted with the FDM/DC method and with the ULM approach. Table I shows the corresponding fitting data considering 20 samples per decade and a convergence tolerance of 0.0001 in the fitting process. In the first stage of the FDM/DC, \mathbf{H} is fitted from 1 Hz to either 10^5 or 10^6 Hz. Then, the error at the LF section is

fitted using 8 poles from 0.001 Hz to 1 Hz. It is mentioned that fitting up to 10^6 Hz gives results very similar to the one up to 10^5 Hz, even with a smaller residue/pole ratio (see Table I). The approximation of $\Delta\mathbf{H}_{LF}$ is shown in Fig. 4. It is observed that deviations of magnitudes are acceptable. The magnitudes of the final approximation for the elements of the first column of \mathbf{H} for the entire frequency range are shown in Fig. 5. It is observed that all the elements are accurately fitted. In ULM, the fitting of \mathbf{H} is performed in a single range of frequencies using four different ranges of frequency (see Table I). It is noticed in Table I that a very large residue/pole ratio results when the frequency range is increased to 8 decades in the ULM, i.e. from 0.001 Hz to 10^5 Hz, and from 0.01 to 10^6 Hz. Moreover, more poles are required with ULM compared to the FDM/DC technique.

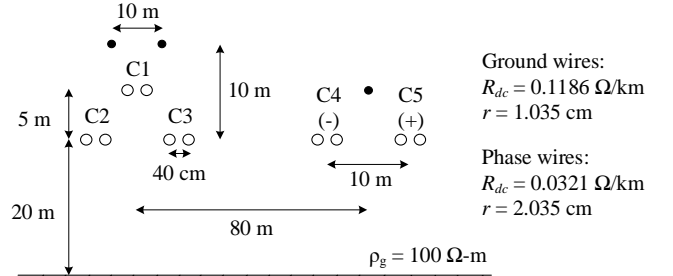


Fig. 3. AC/DC lines geometry.

TABLE I
FITTING DATA OF THE SYSTEM OF FIG. 3

Model	F_{min} (Hz)	F_{max} (Hz)	No. poles (4 groups)	Maximum residue/pole ratio
FDM/DC	0.001	10^5	32	25.23
	0.001	10^6	32	1.46
ULM	0.100	10^5	34	5.17
	0.010	10^5	37	3.85
	0.001	10^5	80	426226.24
	0.010	10^6	100	1633120.74

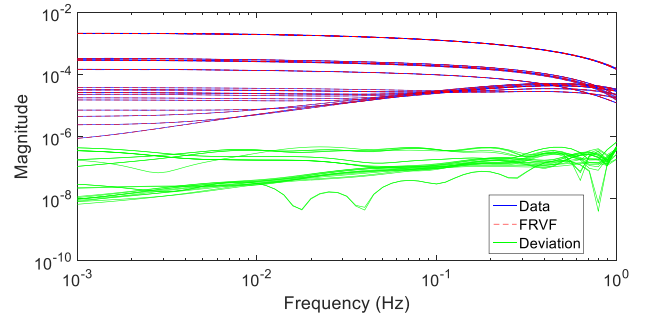


Fig. 4. Low-frequency approximation of function error for $\Delta\mathbf{H}_{LF}$.

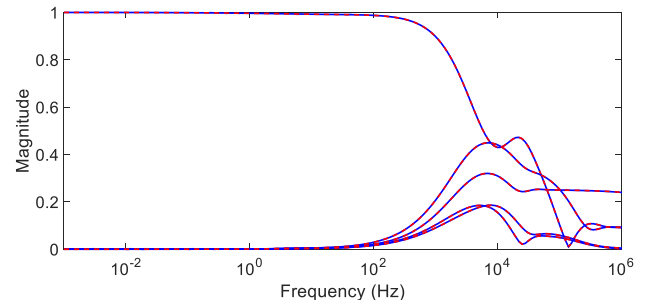


Fig. 5. Magnitude of the first column of \mathbf{H} . Solid line corresponds to actual values while dash lines corresponds to fitted values with FDM/DC.

The two circuit configurations of Fig. 6 are used to test the system of Fig. 3. In the first test (Fig. 6a), a unit step current, with a ramping time of 0.5 s, is applied to the sending end of the positive conductor of the DC line, while the other conductors are grounded. Fig. 7 shows the induced voltage at the receiving end of C2 considering four cases listed in Table I. It is observed that the FDM/DC provides a stable and precise time-domain solution. On the other hand, two ULM cases deviate from the correct response, i.e., cases using minimum frequency values of 0.1 and 0.001 Hz. The computation of accurate DC response requires inclusion of very low frequencies in the fitting of \mathbf{H} ; thus, fitting from 0.1 Hz is not enough. However, reducing the frequency range to 0.001 Hz results in large residue/pole ratios (see Table I), leading to an unstable solution as shown in Fig. 7. This problem is avoided in ULM by setting the minimum frequency for the fitting to 0.01 Hz. In this case, the time-domain response becomes stable and agrees with the solution obtained by the FDM/DC (Fig. 7). However, the ULM requires five poles more than FDM/DC in the fitting of \mathbf{H} (see Table I). Note that the maximum frequency must be adjusted in ULM to provide accurate DC response. Such frequency is not known beforehand and implies a trial-and-error procedure for the common ULM user. On the contrary, the FDM/DC works well with either 10^5 Hz or 10^6 Hz as maximum fitting frequency.

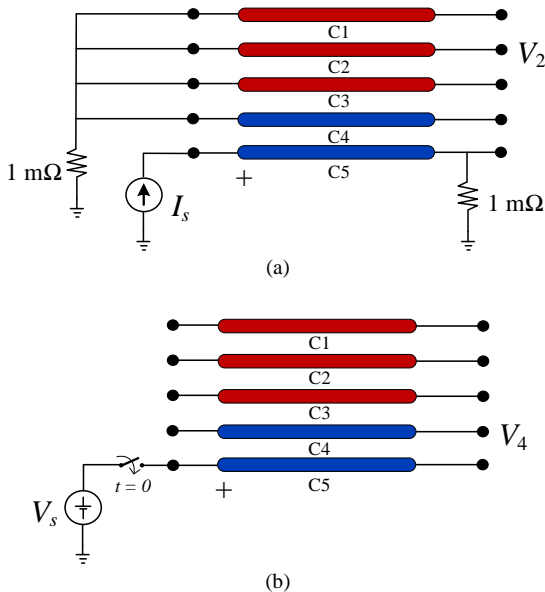


Fig. 6. (a) short- and (b) open-circuit configuration for testing the AC/DC transmission line.

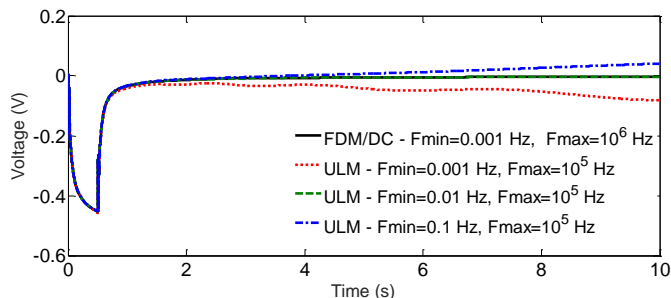


Fig. 7. Time domain results of V_2 in Fig. 6a.

To analyze the performance of the proposed FDM/DC method in a fast front transient, the open-circuit configuration of Fig. 6b is tested. In this second test, a step function is applied to the positive conductor (C5) at the sending end while the receiving end is open. Conductors C1-C4 are left open at both ends. Fig. 8 shows the time-domain results of the induced voltage at the receiving end of C4, i.e. V_4 . The minimum frequency for the fitting in FDM/DC and ULM is set to 0.001 Hz and 0.01 Hz, respectively. It is observed that FDM/DC provides accurate and stable solution regardless F_{\max} , which confirms that the higher frequencies are also accurately simulated. It is noticed that ULM becomes unstable when the frequency range is extended to 1 MHz. The instability problem is due to the resulting very large residue/pole ratio in the fitting of \mathbf{H} (Table I).

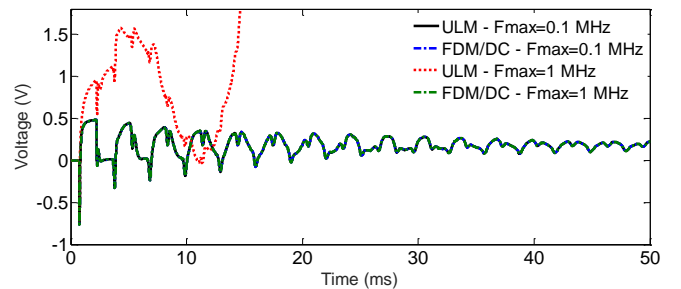


Fig. 8. Time domain results of V_4 in Fig. 6b, time-step 1 μ s.

B. Underground Cable System

This example aims at verifying the precision of FDM/DC and ULM models for computing DC steady-state waveforms in the time-domain simulation of cables. Consider the 4-conductor cable system of Fig. 9 with parameters listed in Table II. For this cable system, \mathbf{H} is fitted with the FDM/DC and ULM approaches. Table III shows the corresponding fitting data. In FDM/DC, the frequency range is partitioned at 1 Hz. In ULM, the identification of \mathbf{H} is performed in a single frequency range considering three different minimum frequency values. It is observed that a less accurate fitting is obtained in ULM when the frequency band used in the fitting is reduced to 0.1 Hz. It is also observed in Table III that when the minimum frequency for the fitting is set to 0.001 Hz, the fitting error (maximum absolute error for the fitting of \mathbf{H}) obtained in ULM is slightly smaller than the one obtained with the FDM/DC; however, ULM requires three more poles. Moreover, the entries of \mathbf{H} identified in ULM are not accurately fitted at low frequencies. Fig. 10 show the magnitude of two entries of \mathbf{H} fitted with FDM/DC and ULM approaches. It is seen that FDM/DC provides accurate fitting, while the entries fitted with ULM show oscillations.

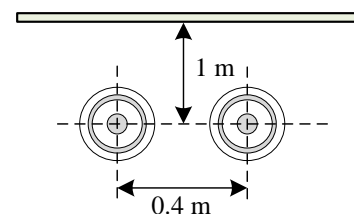


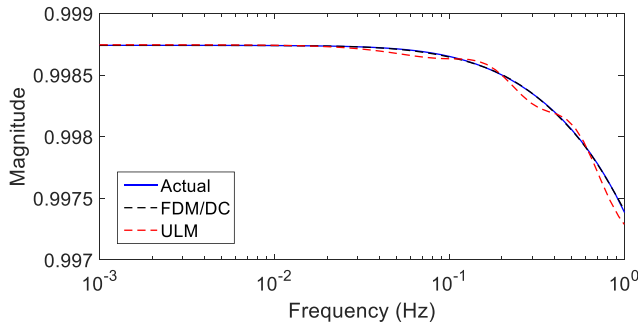
Fig. 9. 4-conductor cable system.

TABLE II
CABLE DATA FOR THE SYSTEM OF FIG. 9

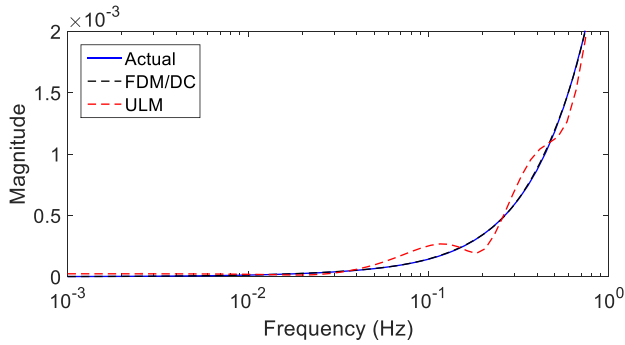
Inner-Outer Radius of the Core	00.00-33.00 mm
Inner-Outer Radius of the Sheath	66.00-66.44 mm
Outer Insulation Radius	76.00 mm
Resistivity of Sheath	1.72×10^{-8} Ohm-m
Resistivity of Core	1.72×10^{-8} Ohm-m
Core Insulator Relative Permittivity	4.10
Shield Insulator Relative Permittivity	2.30
Insulation Loss Factor	0.001
Earth Resistivity	100 Ohm-m

TABLE III
FITTING DATA OF THE SYSTEM OF FIG. 9

Model	F_{\min} (Hz)	F_{\max} (Hz)	No. poles (3 groups)	Max. absolute error for fitting \mathbf{H}
FDM/DC	0.001	10^5	36	0.0044463
ULM	0.001	10^5	39	0.0037779
	0.010		45	0.0088199
	0.100		60	0.0113090



(a)



(b)

Fig. 10. Magnitude of (a) $\mathbf{H}(1,1)$ and (b) $\mathbf{H}(4,1)$ fitted with FDM/DC and ULM approaches.

To see the impact of fitting precision at low frequencies in time domain simulations, especially for induced voltages, the test circuit of Fig. 11 is considered. A unit step voltage is applied to the sending end of the first core, while the sheaths are left open at both ends. For this test, the system of Fig. 9 is modeled with the approaches listed in Table III. Fig. 12 and Fig. 13 show the time-domain voltage V_1 and V_4 (see Fig. 11), respectively. It is observed that there are no significant differences between the responses obtained with FDM/DC and ULM approaches in V_1 , see Fig. 12. However, significant deviations can be observed in the induced sheath voltage V_4 shown in Fig. 13. The FDM/DC provides a steady-state waveform, while the three responses obtained with ULM show

oscillations. It is mentioned that similar results are obtained when the fitting frequency range is increased. Fig. 14 shows the time domain voltage V_4 when the maximum frequency for the fitting is set to 10^6 Hz.

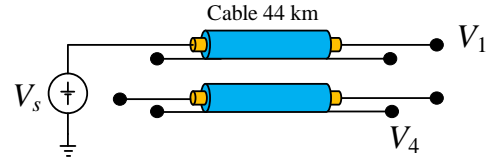


Fig. 11. Test circuit configuration.

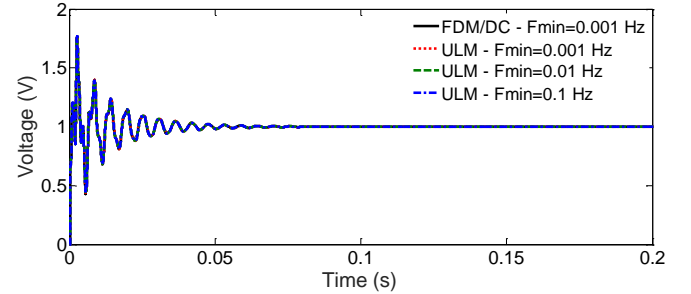


Fig. 12. Time domain results of V_1 in Fig. 11. $F_{\max} = 10^5$ Hz.

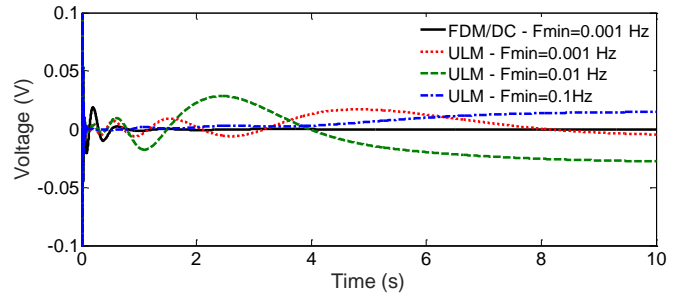


Fig. 13. Time domain results of V_4 in Fig. 11. $F_{\max} = 10^5$ Hz.

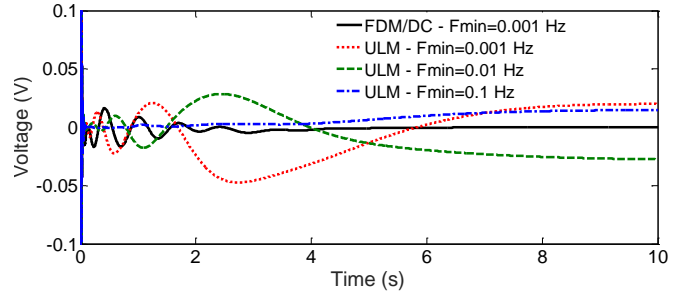


Fig. 14. Time domain results of V_4 in Fig. 11. $F_{\max} = 10^6$ Hz.

V. CONCLUSIONS

This paper presents further details of a recently proposed enhanced fitting procedure for the identification of the propagation function in transmission lines and cables, aimed to reduce the fitting errors at low frequencies. The fitting is performed in a two-stage fashion ensuring precise fitting primarily at frequencies near DC. This approach complements the prevailing universal line model by avoiding numerical instabilities due to large residue/pole ratios, and by improving the accuracy in the computation of DC steady-state waveforms. The accuracy of the new approach is demonstrated via two new test cases.

VI. REFERENCES

- [1] E. V. Larsen, R. A. Walling, and C. J. Bridenbaugh, "Parallel AC/DC transmission lines steady-state induction issues," *IEEE Trans. Power Del.*, vol. 4, no. 1, pp. 667–674, Jan. 1989.
- [2] R. Verdolin, A. M. Gole, E. Kuffel, N. Diseko, and B. Bisewski, "Induced overvoltages on an AC-DC hybrid transmission system," *IEEE Trans. Power Del.*, vol. 10, no. 3, pp. 1514–1524, Jul. 1995.
- [3] B. Gustavsen, G. Irwin, R. Mangerlod, D. Brandt, and K. Kent, "Transmission line models for the simulation of interaction phenomena between parallel AC and DC overhead lines," International Conference on Power System Transients (IPST), Budapest, Hungary, 1999.
- [4] O. M. K. K. Nanayakkara, A. D. Rajapakse, and R. Wachal, "Location of DC Line Faults in Conventional HVDC Systems with Segments of Cables and Overhead Lines Using Terminal Measurements," *IEEE Trans. on Power Del.*, vol. 27, pp. 279–288, 2012.
- [5] A. Morched, B. Gustavsen, and M. Tartibi, "A universal line model for accurate calculation of electromagnetic transients on overhead lines and cables," *IEEE Trans. Power Del.*, vol. 14, no. 3, pp. 1032–1038, Jul. 1999.
- [6] B. Gustavsen and A. Semlyen, "Rational Approximations of Frequency Domain Responses by Vector Fitting," *IEEE Trans. on Power Del.*, vol. 14, pp. 1052–1061, 1999.
- [7] H. M. J. De Silva, A. M. Gole, and L. M. Wedepohl, "Accurate electromagnetic transient simulations of HVDC cables and overhead transmission lines," International Conference on Power System Transients (IPST), Lyon, France, 2007.
- [8] A. Ramirez and R. Iravani, "Enhanced fitting to obtain an accurate dc response of transmission lines in the analysis of electromagnetic transients," *IEEE Trans. Power Del.*, vol. 29, no. 6, pp. 2614–2621, Dec. 2014.
- [9] M. Cervantes, I. Kocar, J. Mahseredjian and A. Ramirez "Partitioned Fitting and DC Correction for the Simulation of Electromagnetic Transients in Transmission Lines/Cables," *IEEE Trans. on Power Del.*, vol. 33, pp. 3246–3248, 2018.
- [10] B. Gustavsen, "Avoiding Numerical Instabilities in the Universal Line Model by a Two-Segment Interpolation Scheme," *IEEE Trans. on Power Del.*, vol. 28, pp. 1643–1651, Jul 2013.
- [11] I. Kocar and J. Mahseredjian, "Accurate Frequency Dependent Cable Model for Electromagnetic Transients," *IEEE Trans. on Power Del.*, vol. 31, pp. 1281–1288, 2016.
- [12] F. J. Marcano and J. R. Marti, "Idempotent line model: Case studies." Proc. of IPST 1997, Seattle, WA. 1997.
- [13] I. Kocar and J. Mahseredjian, "New Procedure for Computation of Time Delays in Propagation Function Fitting for Transient Modeling of Cables," *IEEE Trans. on Power Del.*, vol. 31, pp. 613–621, 2016.
- [14] T. Noda, "Application of frequency-partitioning fitting to the phase-domain frequency-dependent modeling of overhead transmission lines," *IEEE Trans. on Power Del.*, vol. 30, no. 1, pp. 174–183, 2015.
- [15] T. Noda, "Application of frequency-partitioning fitting to the phase-domain frequency-dependent modeling of underground cables," *IEEE Trans. on Power Del.*, vol. 31, no. 4, pp. 1776–1777, 2016.